Porosity Evolution of Activated Carbon Fiber Prepared from Liquefied Wood. Part II: Water Steam Activation from 850 to 950 °C

Zhi Jin and Guangjie Zhao*

To acquire activated carbon fiber from phenol-liquefied wood (PLWACF) with better developed pore structure and a high proportion of mesoporosity, the porosity evolution of PLWACF activated at temperatures from 850 to 950 °C by water steam was detected by the physical adsorption of N_2 at -196 °C. Results showed that the pore structure was well developed by prolonging the activation time at 850 to 910 °C, and it was easy to obtain PLWACF having exceptionally high surface area (larger than 2560 m^2 g^{-1}). However, PLWACF with a specific surface area larger than 3000 m^2 g^{-1} could only be obtained in the late activation stages from 850 to 880 °C. Using this activation process, the mesoporosity was remarkably developed. The mesopore proportion drastically increased with an increase in activation temperature or time, reaching a maximum of 49.5%. The pore size distribution widened as the activation time increased and appeared to accelerate with the use of a higher activation temperature. The mesopore size distribution was enlarged from 2.8 to 5.8 nm.

Keywords: Liquefied wood; Activated carbon fibers; Activation temperature; Porosity evolution; Mesoporosity

*Contact information: College of Material Science and Technology, Beijing Forestry University, Beijing 100083, China; *Corresponding author: zhaows@bjfu.edu.cn*

INTRODUCTION

Activated carbon fiber (ACF) has attracted the attention of chemists and material scientists due to a commercial interest in applications of chemical separation and heterogeneous catalysis; there is also interest in its use as an energy storage material because of its well-developed pore structure (Suzuki 1994; Huang *et al.* 2008; Im *et al.* 2009; Xu *et al.* 2010). The importance of mesoporosity in ACF has also been recognized. ACFs that have a high amount of mesopores are believed to be superior for constructing electric double layer capacitors (Xu *et al.* 2010) and can also aid in the adsorption of large molecules such as hydrogen sulfide (Bashkova *et al.* 2007). Several approaches have been examined to enhance the mesopore region in ACF, *e.g.*, catalysts or polymer additives that are added to the carbon source can increase the pore size distribution (PSD) in ACF (Oya *et al.* 1995; Ozaki *et al.* 1997). However, there are some disadvantages, such as complex processes, costly additives, and ionic impurity.

In the ACF preparation procedure, the activation process plays an important role in determining the porosity of ACF. The partial gasification of the precursor fiber with oxidant gases (such as water steam, carbon dioxide, oxygen, or air) is known as the gas activation method. During the gas activation process, the activation temperature greatly affects the gasification rate, and this influences the porosity development in ACF

(Rodríguez-Reinoso *et al.* 2000). Generally, an increase in the activation temperature produces a larger specific surface area and enhances the total pore volume (Carrott *et al.* 2001; Park and Kim 2001). For example, by carbonization and water steam activation, the Brunauer–Emmett–Teller (BET) specific surface area (S_{BET}) and total pore volume (V_t) of phenolic resin-based ACFs were increased from 628 to 1740 m^2 g^{-1} and 0.346 to 0.937 cm^3 g^{-1}, respectively, with an increase in activation temperature from 750 to 900 °C at an activation time of 30 min. For viscose rayon-based ACF, these quantities were enhanced from 1310 to 2280 m^2 g^{-1} and from 0.694 to 1.40 cm^3 g^{-1}, respectively, by increasing the activation temperature from 850 to 900 °C, with an activation time of 60 min (Naik *et al.* 2011). Conclusively, activating ACF at a higher activation temperature can lead to a reduction in the microporosity and a higher proportion of wide micropores and mesopores, which contributes to the surface area, thus compensating for the decrease in surface area caused by the loss of narrow microporosity (Berger *et al.* 1976; Yang and Yu 1998).

Recently, ACF from PLW has been prepared (Liu and Zhao 2012; Jin and Zhao 2014; Ma *et al.* 2014). Part I of this work has shown that the enhancements in the S_{BET} and V_t of PLWACF activated with water steam is more dependent on the activation time as the activation temperature increases from 650 to 800 °C. The development of the mesoporosity becomes noteworthy only by activation at 800 °C for longer than 100 min, with the mesopore volume reaching a maximum of 0.545 cm^3 g^{-1} (Jin and Zhao 2014). It is thought that PLWACF with larger S_{BET} and V_t as well as a higher proportion of mesoporosity can be obtained by a series of activation processes with water steam at a temperature higher than 800 °C.

To acquire PLWACF with better and more developed pore structure as well as a higher proportion of mesoporosity by only controlling the activation temperature and the activation time, we attempted to study the porosity evolution of PLWACF with water steam at activation temperatures ranging from 850 to 950 °C in this study.

EXPERIMENTAL

Materials

The preparation of phenol-liquefied wood (PLW), synthesis of the PLW spinning solution, and preparation of PLW precursor fibers (the dried fiber after curing and washing with deionized water, which was ready to be carbonized and then activated) proceeded as mentioned in Part I of this work (Jin and Zhao 2014). Aliquots of approximately 5 g of the PLW precursor fiber were each heated at a constant rate in a nitrogen stream to 850, 880, 910, and 950 °C and then activated at the corresponding activation temperature for different activation times by introducing water steam mixed with a nitrogen stream. Finally, they were cooled to room temperature in a nitrogen stream. The PLWACF samples were labeled as "activation temperature (°C)-activation time (min)". For example, 850-20 corresponds to PLWACF prepared by an activation stage at 850 °C for 20 min.

Methods

The burn-off, which is defined as the difference between the mass before and after activation, was calculated as follows

$$\text{Burn-off} = (w_0\text{-}w_1)/w_0 \times 100\% \quad (1)$$

where w_0 and w_1 are the mass of the carbonized fiber before and after activation, respectively.

Nitrogen adsorption/desorption isotherms were collected at -196 °C by an automatic adsorption system (Autosorb-iQ, Quantachrome, USA) to study the porous characteristics of the prepared PLWACF. Before each measurement, the samples were degassed at 300 °C for 3 h. S_{BET} was then calculated using the BET method (Brunauer *et al.* 1938). The micropore specific surface area was determined using the t-plot micropore analysis method (Deboer *et al.* 1966). V_t was calculated from the nitrogen volume adsorbed at the maximum value of relative pressure, P/P_0. The micropore volume (V_{mi}) and mesopore volume (V_{me}) were determined by using quenched solid density functional theory (QSDFT) method (Lastoskie *et al.* 1993). The PSDs in the micropore and mesopore region were determined using Horvath–Kawazoe (HK) method and the Barrett-Joyner-Halenda (BJH) method, respectively. All samples were examined three times, and the obtained results were within the accepted error range of 5%.

RESULTS AND DISCUSSION

Changes in Burn-off

Figure 1 shows the variations in burn-off during the activation at 850 to 950 °C as a function of activation time. As can be seen, the burn-off value of PLWACF continuously increased with prolonged activation time or increased activation temperature, ranging from 15% to 95%. The burn-off values for samples 850-220, 880-140, 910-100, and 950-60 were all almost equal, reaching a maximum of almost 95%. Volatile matter emitted when the carbon source is subject to attacks from the activator (water steam) is more easily released from the carbon matrix with the augment of activation temperature from 850 to 950 °C (Carrott *et al.* 2001).

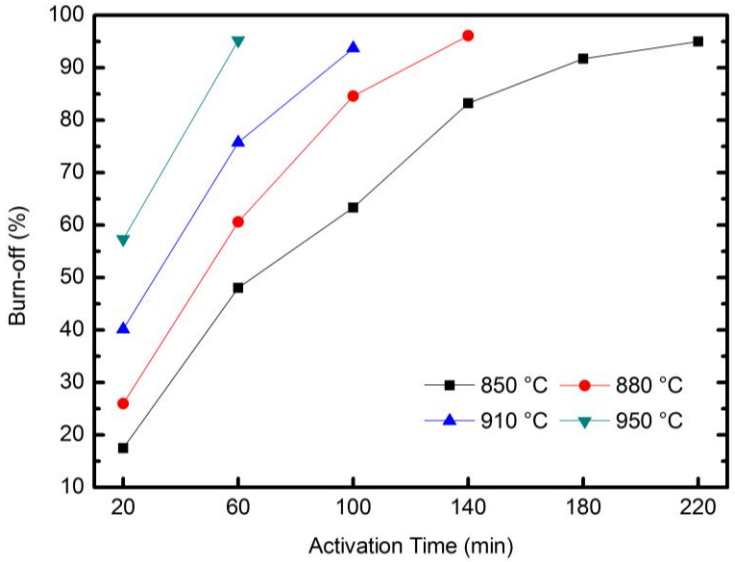

Fig. 1. Changes in burn-off of PLWACF

Pore Structure Evolution

Figure 2 describes the typical N_2-adsorption/desorption isotherms for PLWACF. All of the adsorption isotherms were of type-I according to the IUPAC classification, which is consistent with micropore absorption. When activated at temperatures from 850 to 950 °C, the knees of the isotherms become wider with increasing activation time, which suggests the formation of larger pores (Lee *et al*. 2003). The nitrogen adsorption capacity increases with an increase in activation time; this shows the development of porosity. Furthermore, a higher activation temperature appears to promote an increase in nitrogen adsorption capacity with increasing activation time.

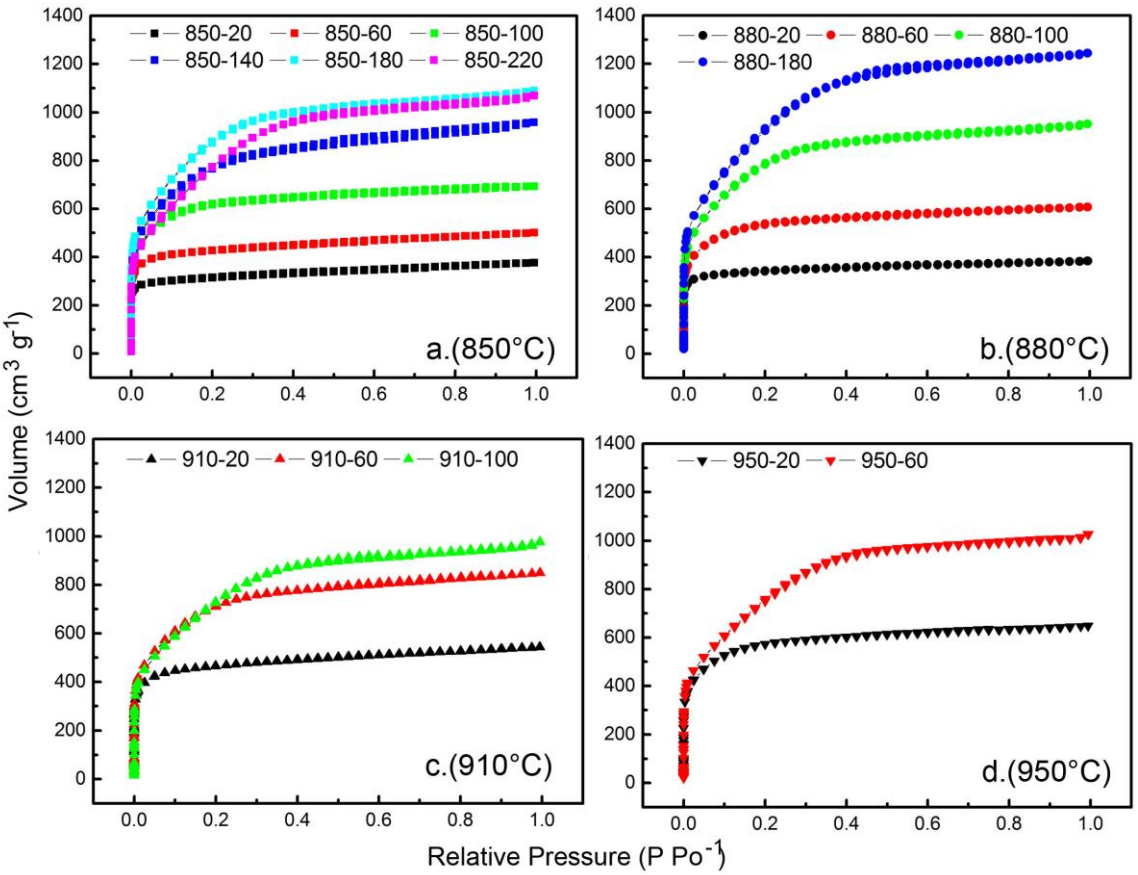

Fig. 2. The nitrogen adsorption/desorption isotherms at -196 °C for the prepared PLWACF

The pore characteristics of all the prepared PLWACF are listed in Table 1. As shown, the S_{BET} and V_t all increased with increasing activation temperature or activation time. As the activation temperature increased, the S_{BET} and V_t progressively increased from 1647 to 2833 m^2 g^{-1} and from 0.775 to 1.589 cm^3 g^{-1}, respectively, when activated for 60 min. With activation at 880 °C for 140 min, the S_{BET} and V_t reached maximum at 3461 m^2 g^{-1} and 1.925 cm^3 g^{-1}, respectively. Typically, ACFs with S_{BET} larger than 2560 m^2 g^{-1} are regarded as exceptionally high-surface area materials, so-called "super ACFs", which are beneficial to applications such as gas storage and supercapacitors (Pandolfo and Hollenkamp 2006; Wang *et al.* 2008). Compared to the results from Part I of this work, water steam activation from 850 to 950 °C more effectively enhanced the S_{BET} than that at 650 to 800 °C, by which the maximum S_{BET} only reached 2410 m^2 g^{-1} (Jin and Zhao 2014). Moreover, it is interesting to see that when compared with 910-100 and 950-

60, 850-140, and 880-100 showed similar S_{BET} values but possessed lower burn-off values. Meanwhile, in the case of 850-180, 850-220, and 880-140, they exhibited high S_{BET} and large V_t values, even though their burn-off values were consistent with those of 910-100 and 950-60. When activated at 850 to 880 °C, the gasification of the carbon matrix and the diffusion of the activator to the inside of the carbon matrix proceed at a suitable rate, making the extent of the activation process more uniform, while activations at temperatures that are too high (910 to 950 °C) lead to a sintering effect, which causes a recession in the pore structure development (Okada *et al.* 2003).

The V_{HK} and V_{BJH} were all enhanced with the increase in the activation temperature or time. The V_{HK} increased gradually with increasing activation temperature at the short activation time of 20 min from 0.478 to 0.862 $cm^3\ g^{-1}$. When the activation time was prolonged to more than 60 min, lower activation temperatures at 850 to 880 °C favored the enhancement in $V_{HK,}$ reaching the maximum at 1.306 $cm^3\ g^{-1}$ in the case of sample 880-140. The increase in V_{BJH} with activation time appeared to accelerate at a higher activation temperature. As an increase of activation time from 20 min to 60 min, the value of V_{BJH} was increased by 1.53 times at 950 °C compared with 22% at 850 °C. The maximum of V_{BJH} was 0.350 $cm^3\ g^{-1}$ in the case of sample 850-220. Thus, it is sure that the pore formation of the prepared PLWACF is dependent on the development in the microporosity as well as mesoporosity simultaneously.

Table 1. Pore Structure Parameters of All the Prepared PLWACF

Sample	S_{BET} ($m^2\ g^{-1}$)	V_t ($cm^3\ g^{-1}$)	S_{mi} ($m^2\ g^{-1}$)	V_{HK} ($cm^3\ g^{-1}$)	V_{BJH} ($cm^3\ g^{-1}$)	V_{mi}/V_t (%)	V_{me}/V_t (%)	V_{me}/V_{mi}
850-20	1221	0.583	1041	0.478	0.107	71.9	21.3	0.296
850-60	1647	0.775	1422	0.650	0.131	70.8	21.7	0.306
850-100	2280	1.073	1996	0.930	0.117	57.0	35.4	0.621
850-140	2788	1.482	2120	1.114	0.283	48.9	43.8	0.896
850-180	3223	1.686	2300	1.250	0.221	51.1	41.1	0.804
850-220	2929	1.654	1389	1.085	0.350	43.5	49.2	1.130
880-20	1340	0.593	1197	0.521	0.074	78.8	14.2	0.180
880-60	1975	0.940	1740	0.805	0.116	58.5	34.0	0.582
880-100	2875	1.471	2100	1.128	0.203	52.5	40.0	0.761
880-140	3461	1.925	1746	1.306	0.331	45.0	48.2	1.070
910-20	1786	0.840	1528	0.708	0.136	68.6	23.7	0.345
910-60	2592	1.313	2089	1.037	0.191	50.7	42.1	0.831
910-100	2714	1.510	1637	1.027	0.252	45.0	47.0	1.043
950-20	2118	1.003	1839	0.862	0.120	56.4	36.1	0.640
950-60	2833	1.589	1302	1.059	0.304	42.7	49.5	1.160

V_{HK}: micropore volume calculated by HK method;
V_{BJH}: mesopore volume calculated by BJH method

It should be noted that with the increase of activation temperature or time, the values of V_{me}/V_t and V_{me}/V_{mi} all were drastically increased, while the value of V_{mi}/V_t was decreased, exhibiting an opposite trend (Fig. 3). Thus, there was clearly a more remarkable development of mesoporosity than of microporosity during the activation process, which was probably a result of the formation of mesopores by the burn-off of walls between adjacent micropores. At the late stage of these four activation processes (with the burn-off larger than 90% as shown in Fig. 1), S_{mi} decreased and the values of V_{me}/V_{mi} exceeded 1. Eventually, V_{me}/V_t reached the maximum of 49.5% compared with the V_{mi}/V_t of 42.7%, which confirms the predominant role of mesoporosity in PLWACF.

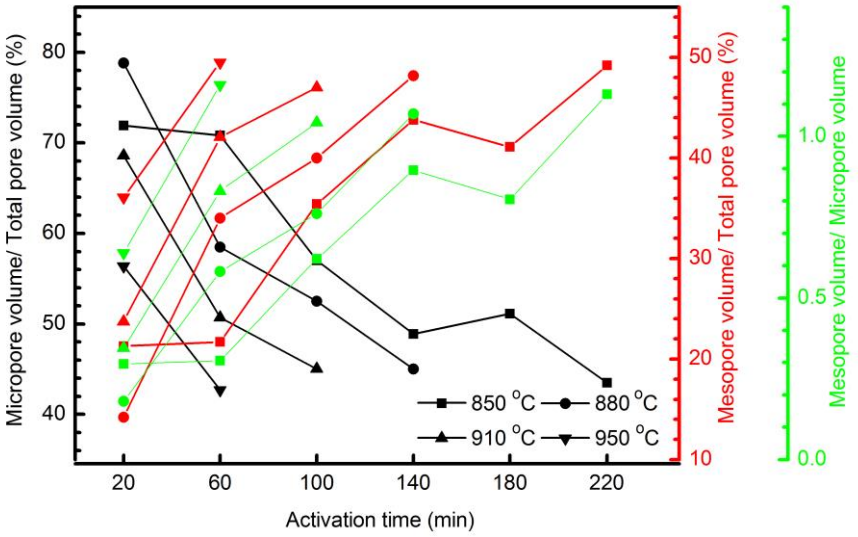

Fig. 3. The evolution of ratios of V_{mi}/V_t, V_{me}/V_t, and V_{me}/V_{mi} of the prepared PLWACF

Micropore size distribution evolution of PLWACF obtained by means of HK method is shown in Fig. 4.

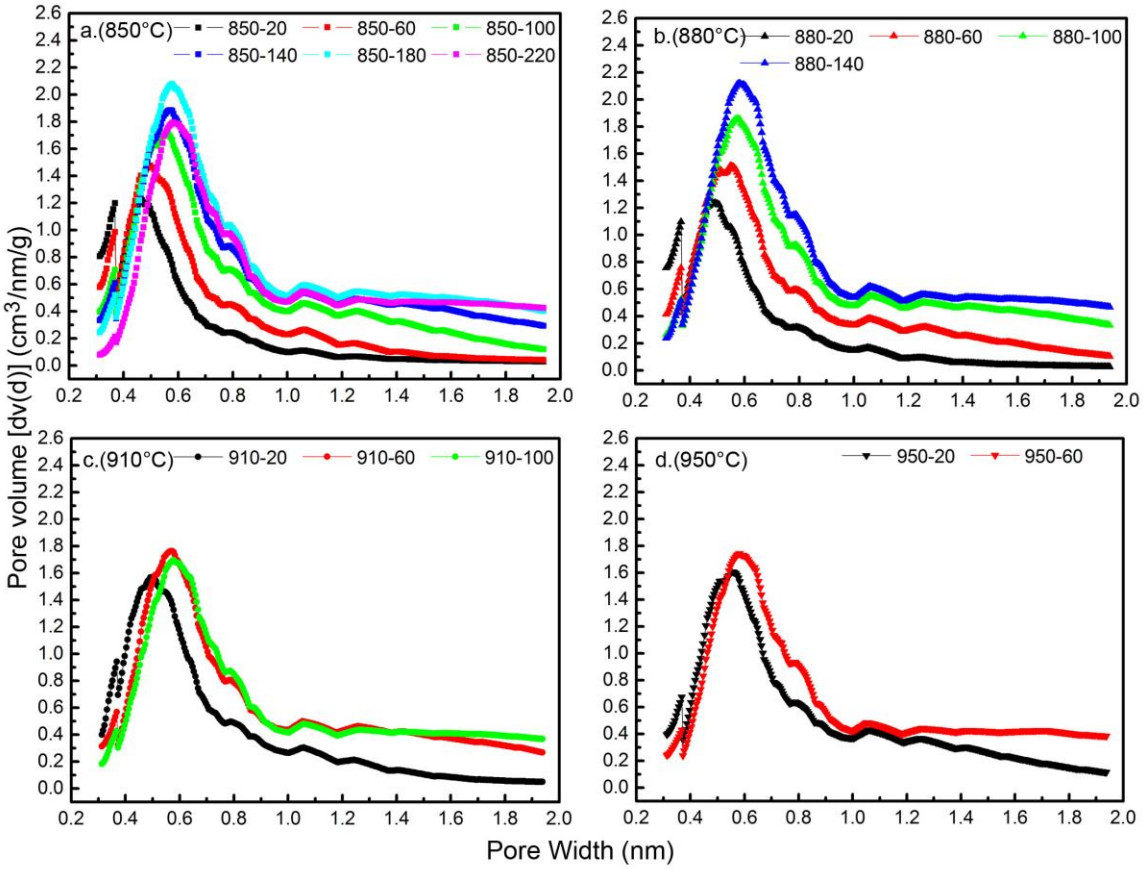

Fig. 4. PSDs obtained by HK method for the prepared PLWACFs

It can be seen that the micropore size distribution was widened in the whole micropore range (0.3 to 2.0 nm) as the activation was proceeding. The PSD maxima calculated by HK method (D_{HK}) are plotted in Fig. 5.

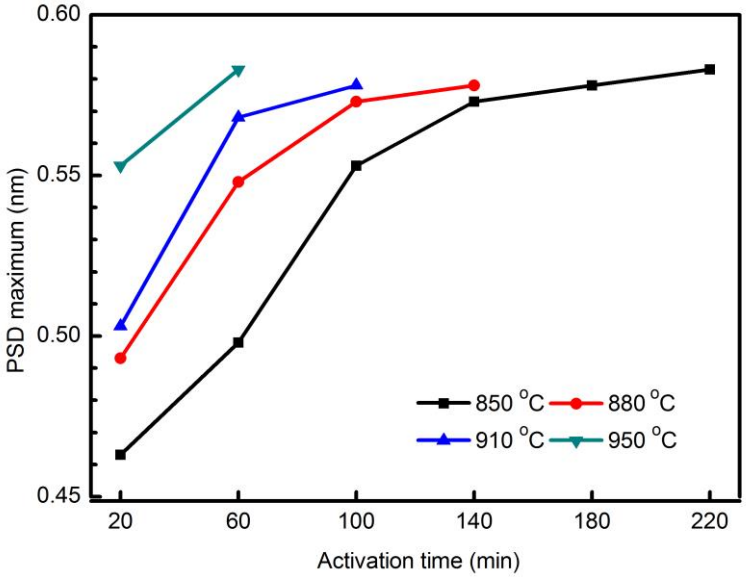

Fig. 5. The evolution of PSD maximum calculated by HK method of the prepared PLWACF

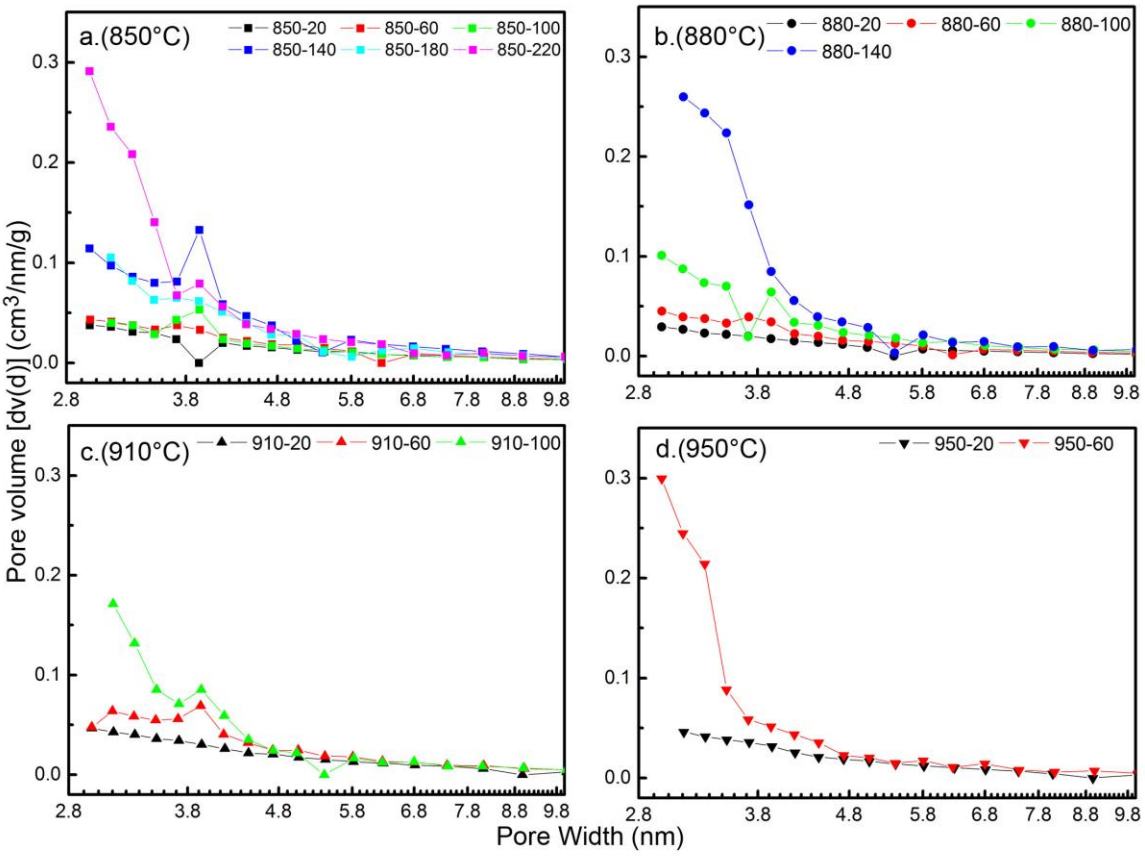

Fig. 6. PSDs obtained by BJH method for the prepared PLWACFs

The value of D_{HK} was progressively increased with the increase of activation temperature or time, showing that the development in the micropore size distribution took place by pore widening in a gradual way as the activation time increased. When activated for 20 min, the D_{HK} was widened from 0.462 nm to 0.552 nm as the activation temperature increased. Moreover, the increase in the D_{HK} became smooth with increasing activation time, and the maximum D_{HK} approached to around 0.580 nm at the late stage of activation at 850 to 950 °C. From this it may be concluded that the enlargement in the micropore size distribution tends to stabilize.

Figure 6 depicts the mesopore size distribution of PLWACF by applying the BJH method, which showed a gradual enlargement of the mesoporosity in the 2.8 to 5.8 nm interval. In the case of samples 850-220, 880-140, 910-100, and 950-60, significant enlargements were observed. However, their D_{HK} values were almost identical (approximately 0.580 nm as shown in Fig. 5). Consequently, these widened mesopores primarily came from the corrosion of the existing smaller pores, which are apparently independent of the development of new pores. It is possible that significant surface erosion and carbon structure shrinkage at 850 to 950 °C made the fiber too thin to sustain the formation of new pores with increasing activation time.

CONCLUSIONS

The porosity evolution of phenol liquefied wood-based activated carbon fiber (PLWACF) with water steam activation at 850 to 950 °C was examined.

1. S_{BET} and V_t increase with increasing activation time at temperatures ranging from 850 to 950 °C. PLWACFs with S_{BET} greater than 3000 m^2 g^{-1} can only be obtained by activation at 850 °C for 180 min and at 880 °C for 140 min, possibly because the gasification of the carbon matrix and the diffusion of the activator proceeded at a suitable rate.
2. The pore formation of the prepared PLWACF is dependent on the development in the microporosity and mesoporosity simultaneously. The amount of microporosity development is relatively mild, and activations at lower temperatures (850 to 880 °C) for longer than 60 min are in favor of larger micropore volume. The mesopore ratio drastically increases as the activation time or activation temperature is increased, showing a remarkable amount of mesoporosity development. At the late stage of activation (with the burn-off larger than 90%), the mesoporosity plays a predominant role, which is evidenced by a significant decrease in the micropore specific surface area and a mesopore volume that exceeds the micropore volume.
3. For all activation temperatures, the widening of the pore size distribution progressively takes place as the activation time increases, which appears to accelerate with the enhancement of the activation temperature. Typically, the mesopore size distribution is enlarged from 2.8 to 5.8 nm. Widened mesopores form during the whole activation process, primarily owing to the corrosion of existing smaller.

ACKNOWLEDGMENTS

The authors are grateful for the support from the Specialized Research Fund for the Doctoral Program of Higher Education, Grant. No. 20130014130001.

REFERENCES CITED

Bashkova, S., Baker, F. S., Wu, X. X., Armstrong, T. R., and Schwartz, V. (2007). "Activated carbon catalyst for selective oxidation of hydrogen sulphide: On the influence of pore structure, surface characteristics, and catalytically-active nitrogen," *Carbon* 45(6), 1354-1363.

Berger, J., Siemieniewska, T., and Tomkov, K. (1976). "Development of porosity in brown-coal chars on activation with carbon dioxide," *Fuel* 55(1), 9-15.

Brunauer, S., Emmett, P. H., and Teller, E. (1938). "Adsorption of gases in multimolecular layers," *J. Am. Chem. Soc.* 60(2), 309-319.

Carrott, P. J. M., Nabais, J. M. V., Carrott, M. M. L. R., and Pajares, J. A. (2001). "Preparation of activated carbon fibres from acrylic textile fibres," *Carbon* 39(10), 1543-1555.

Deboer, J. H., Lippens, B. C., Linsen, B. G., Broekhof, J. C., Vandenhe, A., and Osinga, T. J. (1966). "T-curve of multimolecular N_2-adsorption," *J. Colloid Interf. Sci*. 21(4), 405-411.

Huang, H. X., Chen, S. X., and Yuan, C. (2008). "Platinum nanoparticles supported on activated carbon fiber as catalyst for methanol oxidation," *J. Power Sources* 175(1), 166-174.

Im, J. S., Jung, M. J., and Lee, Y. S. (2009). "Effects of fluorination modification on pore size controlled electrospun activated carbon fibers for high capacity methane storage," *J. Colloid Interf. Sci.* 339(1), 31-35.

Jin, Z., and Zhao, G. (2014). "Porosity evolution of activated carbon fiber prepared from liquefied wood. Part I: Water steam activation at 650 to 800° C," *BioResources* 9(2), 2237-2247.

Lastoskie, C., Gubbins, K. E., and Quirke, N. (1993). "Pore-size distribution analysis of microporous carbons - A density-functional theory approach," *J. Phys. Chem.* 97(18), 4786-4796.

Lee, Y. S., Basova, Y. V., Edie, D. D., Reid, L. K., Newcombe, S. R., and Ryu, S. K. (2003). "Preparation and characterization of trilobal activated carbon fibers," *Carbon* 41(13), 2573-2584.

Liu, W., and Zhao, G. (2012). "Effect of temperature and time on microstructure and surface functional groups of activated carbon fibers prepared from liquefied wood," *BioResources* 7(4), 5552-5567.

Ma, X. J., Zhang F., Zhu J. Y., Yu L. L., and Liu X. Y. (2014). "Preparation of highly developed mesoporous activated carbon fiber from liquefied wood using wood charcoal as additive and its adsorption of methylene blue from solution," *Bioresour Technol*. 164, 1-6.

Naik, J. R., Bikshapathi, M., Singh, R. K., Sharma, A., Verma, N., Joshi, H. C., and Srivastava, A. (2011). "Preparation, surface functionalization, and characterization of carbon micro fibers for adsorption applications," *Environ. Eng. Sci.* 28(10), 725-733.

Okada, K., Yamamoto, N., Kameshima, Y., and Yasumori, A. (2003). "Porous properties of activated carbons from waste newspaper prepared by chemical and physical activation," *J. Colloid Interf. Sci.* 262(1), 179-193.

Oya, A., Yoshida, S., Alcaniz-Monge, J., and Linares-Solano, A. (1995). "Formation of mesopores in phenolic resin-derived carbon fiber by catalytic activation using cobalt," *Carbon* 33(8), 1085-1090.

Ozaki, J., Endo, N., Ohizumi, W., Igarashi, K., Nakahara, M., and Oya, A. (1997). "Novel preparation method for the production of mesoporous carbon fiber from a polymer blend," *Carbon* 35(7), 1031-1033.

Park, S. J., and Kim, K. D. (2001). "Influence of activation temperature on adsorption characteristics of activated carbon fiber composites," *Carbon* 39(11), 1741-1746.

Pandolfo, A. G., and Hollenkamp, A. F. (2006). "Carbon properties and their role in supercapacitors," *J. Power Sources* 157(1), 11-27.

Rodríguez-Reinoso, F., Pastor, A. C., Marsh, H., and Martínez, M. A. (2000). "Preparation of activated carbon cloths from viscous rayon. Part II: Physical activation processes," *Carbon* 38(3), 379-395.

Suzuki, M. (1994). "Activated carbon fiber: Fundamentals and applications," *Carbon* 32(4), 577-586.

Wang, J. F., Gu, J. L., Han, X. J., and Wang, Y. X. (2008). "The study of phenolic resin-based mesopore activated carbon with superhigh specific surface area," *Carbon* 3, 20-23.

Xu, B., Wu, F., Chen, R., Cao, G., Chen, S., and Yang, Y. (2010). "Mesoporous activated carbon fiber as electrode material for high-performance electrochemical double layer capacitors with ionic liquid electrolyte," *J. Power Sources* 195(7), 2118-2124.

Yang, M. C., and Yu, D. G. (1998). "Influence of activation temperature on the properties of polyacrylonitrile-based activated carbon hollow fiber," *J. Appl. Polym. Sci.* 68(8), 1331-1336.

Article submitted: May 4, 2014; Peer review completed: August 1, 2014; Revised version received and accepted: August 21, 2014; Published: September 26, 2014.